



HAL
open science

Efficiency of sympagic-benthic coupling revealed by analyses of n-3 fatty acids, IP 25 and other highly branched isoprenoids in two filter-feeding Arctic benthic molluscs: *Mya truncata* and *Serripes groenlandicus*

Rémi Amiraux, Philippe Archambault, Brivaëla Moriceau, Mélanie Lemire, Marcel Babin, Laurent Mémery, Guillaume Massé, Jean-Eric Tremblay

► **To cite this version:**

Rémi Amiraux, Philippe Archambault, Brivaëla Moriceau, Mélanie Lemire, Marcel Babin, et al.. Efficiency of sympagic-benthic coupling revealed by analyses of n-3 fatty acids, IP 25 and other highly branched isoprenoids in two filter-feeding Arctic benthic molluscs: *Mya truncata* and *Serripes groenlandicus*. *Organic Geochemistry*, 2020, 10.1016/j.orggeochem.2020.104160 . hal-03019232

HAL Id: hal-03019232

<https://hal.science/hal-03019232>

Submitted on 23 Nov 2020

HAL is a multi-disciplinary open access archive for the deposit and dissemination of scientific research documents, whether they are published or not. The documents may come from teaching and research institutions in France or abroad, or from public or private research centers.

L'archive ouverte pluridisciplinaire **HAL**, est destinée au dépôt et à la diffusion de documents scientifiques de niveau recherche, publiés ou non, émanant des établissements d'enseignement et de recherche français ou étrangers, des laboratoires publics ou privés.

Journal Pre-proofs

Efficiency of sympagic-benthic coupling revealed by analyses of n-3 fatty acids, IP₂₅ and other highly branched isoprenoids in two filter-feeding Arctic benthic molluscs: *Mya truncata* and *Serripes groenlandicus*

Rémi Amiriaux, Philippe Archambault, Brivaela Moriceau, Mélanie Lemire, Marcel Babin, Laurent Memery, Guillaume Massé, Jean-Eric Tremblay

PII: S0146-6380(20)30195-9
DOI: <https://doi.org/10.1016/j.orggeochem.2020.104160>
Reference: OG 104160

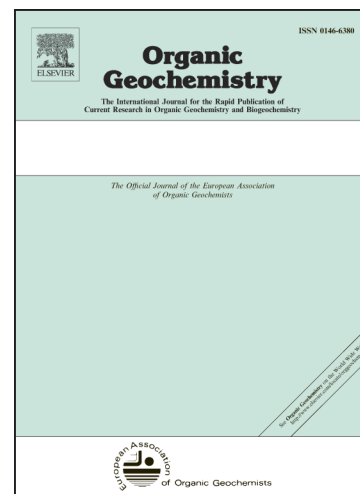
To appear in: *Organic Geochemistry*

Received Date: 13 August 2020
Revised Date: 3 November 2020
Accepted Date: 9 November 2020

Please cite this article as: Amiriaux, R., Archambault, P., Moriceau, B., Lemire, M., Babin, M., Memery, L., Massé, G., Tremblay, J-E., Efficiency of sympagic-benthic coupling revealed by analyses of n-3 fatty acids, IP₂₅ and other highly branched isoprenoids in two filter-feeding Arctic benthic molluscs: *Mya truncata* and *Serripes groenlandicus*, *Organic Geochemistry* (2020), doi: <https://doi.org/10.1016/j.orggeochem.2020.104160>

This is a PDF file of an article that has undergone enhancements after acceptance, such as the addition of a cover page and metadata, and formatting for readability, but it is not yet the definitive version of record. This version will undergo additional copyediting, typesetting and review before it is published in its final form, but we are providing this version to give early visibility of the article. Please note that, during the production process, errors may be discovered which could affect the content, and all legal disclaimers that apply to the journal pertain.

© 2020 Published by Elsevier Ltd.



Efficiency of sympagic-benthic coupling revealed by analyses of n-3 fatty acids, IP₂₅ and other highly branched isoprenoids in two filter-feeding Arctic benthic molluscs: *Mya truncata* and *Serripes groenlandicus*

Rémi Amiraux^{a, b*}, Philippe Archambault^{a, c}, Brivaela Moriceau^b, Mélanie Lemire^d, Marcel Babin^a, Laurent Memery^b, Guillaume Massé^a, Jean-Eric Tremblay^a

^a Takuvik International Research Laboratory, Québec Océan, Laval University (Canada) - CNRS, Département de biologie and Québec-Océan, Université Laval, Québec, Québec, Canada

^b Laboratoire des Sciences de l'Environnement MARin (LEMAR), UMR 6539 CNRS/Ifremer/IRD/UBO, Institut Universitaire Européen de la Mer (IUEM), Technopôle Brest-Iroise, Plouzané, France

^c ArcticNet, Québec Océan, Département de Biologie, Université Laval, Quebec, QC, Canada

^d Axe santé des populations et pratiques optimales en santé, Centre de recherche du CHU de Québec, Université Laval, Québec, Canada

*Correspondence to: R. Amiraux (remi.amiraux@takuvik.ulaval.ca); Tel.: +1 418 440 3276

Abstract

The aim of this work was to determine the impact of sympagic (ice-associated) algal primary production on the quality of Arctic filter-feeding bivalves. For this purpose, we investigated the sea ice production of lipids (including omega-3 polyunsaturated fatty acids (n-3 PUFA) and highly branched isoprenoids (HBI)), as well as their subsequent incorporation into the truncate softshell clam (*Mya truncata*) and the Greenland cockle (*Serripes groenlandicus*) during the melting periods of two consecutive years in Baffin Bay. Lipid and primary production exhibited seasonal variability and overall contrasts between the two years as a result of distinct physical forcings and the ensuing biological responses. Whilst less productive in terms of total lipids or chlorophyll *a*, Spring 2016 was more productive than Spring 2015 for n-3 PUFA, which are essential for benthic fauna. The sea ice diatom HBI biomarker IP₂₅ was quantified in sea ice from both years. Interestingly, such production was preceded by a production of the hitherto ‘pelagic’ biomarker, HBI III, in sea ice. In bivalves, HBI contents and correlations confirmed the tightness of the Arctic sympagic-benthic coupling and highlighted that *S. groenlandicus* can be used as a sentinel species for assessing the degree of this coupling. The confirmation that bivalves incorporate sea-ice derived HBI III and not only IP₂₅, may introduce uncertainties into the use of some HBI-based indices. Monitoring of the fatty acid contents of bivalves allowed identification of their spawning periods and suggests that *M. truncata* did not store enough n-3 PUFA to sustain its reproductive effort.

Keywords: Arctic shelves; Sympagic-benthic coupling; IP₂₅; HBI; n-3 PUFA; EPA; DHA; *Mya truncata*; *Serripes groenlandicus*; ice-derived HBI III;

1. Introduction

Arctic marine food webs are classically viewed as being supported by two ecologically distinct types of primary production effected in sequence by sympagic (ice-associated) algae and pelagic (water column) algae or phytoplankton (Gosselin et al., 1997; Horner and Schrader, 1982; Pabi et al., 2008; Wassmann et al., 2011). Among the essential organic molecules produced by algae, omega-3 polyunsaturated fatty acids (n-3 PUFA), such as eicosapentaenoic acid (EPA) 20:5(n-3) and docosahexaenoic acid (DHA) 22:6(n-3), are considered as highly relevant indicators of nutritional value for consumers (Hendriks et al., 2003). These specific lipids are produced almost exclusively by algae and are necessary for the whole food web, from primary consumers (e.g., bivalves) to top predators and even human populations. As algal species differ in their lipid production and more specifically in their PUFA contents (Leonardos and Lucas, 2000; Napolitano et al., 1990; Volkman et al., 1989), it is not surprising that EPA and DHA derive from different sources of primary production. Indeed, EPA is mostly produced by diatoms, a dominant taxon of both sympagic and pelagic algae (Kelly and Scheibling, 2012; Poulin et al., 2011; Viso and Marty, 1993), while DHA is associated with dinoflagellates, a mostly pelagic taxon (Kelly and Scheibling, 2012; Poulin et al., 2011; Søreide et al., 2008).

Sympagic and pelagic contributions to total primary production are highly variable depending on the season and the region, but it is generally admitted that sympagic algae contribute less than phytoplankton to annual primary production (Dupont, 2012; Fernández-Méndez et al., 2015). In contrast, sympagic primary production is recognized as an important contributor of carbon (C) exported towards the seafloor (Boetius et al., 2013; McMahon et al., 2006). This strong contribution results from the high sinking rates of ice-algal cells or aggregates (Boetius et al., 2013; Riebesell et al., 1991) and their good preservation during transit (Amiriaux et al., 2017; Amiriaux et al., 2020). In contrast, phytoplankton have a longer residence time in the water column due to their slow sinking rates (van der Loeff et al., 2002),

which can lead to higher bacterial degradation and can reduce the quality of algal material reaching the seafloor (Morata and Renaud, 2008; Roy et al., 2015). It is therefore not surprising that the essential fatty acid content of this material is relatively high when it derives from sea ice (Falk-Petersen et al., 1998; McMahon et al., 2006; Sun et al., 2009; Wang et al., 2014). On this basis, sympagic algae are considered as a prime food source for benthic consumers that depend on these fatty acids for growth and reproduction (Lovvorn et al., 2005; McMahon et al., 2006; North et al., 2014).

Determining the impact of each primary production source on the quality of food for the benthic community requires an estimation of their relative contributions. Several approaches have been employed for estimating these contributions (e.g., stable isotopes and fatty acid biomarkers; Gaillard et al., 2017; Gaillard et al., 2015). Among these, quantification of highly branched isoprenoid (HBI) alkenes has provided robust estimates of the relative share of different microalgal primary production sources in consumer biomass (Brown et al., 2017; Brown and Belt, 2012). In recent years, the development of HBI-based proxies has highlighted the relatively high source-specificity of a number of these molecules. Among these, IP₂₅ (Ice Proxy with 25 carbon atoms; Belt et al., 2007) is a mono-unsaturated C₂₅ HBI (**Fig. 1**) which seems to be produced exclusively by certain Arctic sympagic diatoms (e.g., *Pleurosigma stuxbergii* var. *rhomboides* (Cleve in Cleve & Grunow) Cleve, *Haslea kjellmanii* (Cleve) Simonsen, *Haslea spicula* (Hickie) Lange-Bertalot; Brown et al., 2014c; Limoges et al., 2018). A close structural analogue of IP₂₅, but with an additional double bond in its structure, is known as HBI IIa (**Fig. 1**) and this co-occurs with IP₂₅ in Arctic sea ice and associated sediments. In a recent study, Belt et al. (2016) identified HBI IIa in the Southern Ocean and showed it to be produced by the sympagic diatom *Berkeleya adeliensis* (Medelin). The authors proposed the term IPSO₂₅ (ice proxy for the Southern Ocean with 25 carbon atoms) for this biomarker, at least when detected in this ocean (Belt et al., 2016). Finally, a third (at least) HBI has been

identified in several *Rhizosolenia* spp. isolated from polar and sub-polar locations (Belt et al., 2017) and has been linked with pelagic primary production under ice-free conditions in both the Arctic and the Antarctic (Belt, 2018; Belt et al., 2015; Collins et al., 2013; Massé et al., 2011). As a common constituent of marine settings (Belt et al., 2000), this tri-unsaturated HBI, sometimes referred to as HBI III (**Fig. 1**), has shown potential as a proxy of pelagic production for the spring marginal ice zone (MIZ) in polar seas (Belt et al., 2019; Collins et al., 2013; Köseoğlu et al., 2018; Smik et al., 2016a; Smik et al., 2016b). More recently, HBI III has also shown potential as a proxy for pelagic productivity associated with arctic sea fronts (Harning et al., 2020).

It is commonly accepted that a large proportion of the sympagic algal biomass released during sea ice melt, sinks to the seafloor, where it provides an important initial C and n-3 PUFA source for benthos growth and reproduction after the food limited winter (McMahon et al., 2006; North et al., 2014). However, to the best of our knowledge, no studies have jointly monitored the temporal evolution of primary production quality (n-3 PUFA) and source (HBIs) in sea ice and the benthic filter-feeders underneath. In order to enhance our understanding of pelagic-benthic coupling in the Arctic, the present study monitored the temporal evolution of n-3 PUFAs and HBIs in sea ice and two benthic filter-feeder bivalve molluscs (*Mya truncata* and *Serripes groenlandicus*) during two melting periods in southwest Baffin Bay. Our objectives were: (i) to determine the seasonal and interannual variability of sea ice high-quality lipid production in sea ice, (ii) to determine the seasonal and interannual enrichment of these lipids in the two bivalve species and (iii) to confirm the use of *M. truncata* and *S. groenlandicus* as indicators of the tightness of pelago-benthic coupling. This study will enhance our understanding of the Arctic pelagic-benthic coupling, as well as highlight the seasonal and annual influences of sea ice lipid production on the quality of bivalves and of their reproductive capacity.

2. Materials and Methods

2.1 Study site and sampling

Sampling was conducted in 2015 and 2016 at a landfast-ice station located near Qikiqtarjuaq Island (**Fig. 2**) in southwest Baffin Bay (Canadian Arctic) within the framework of the GreenEdge project. Sea ice sampling was conducted every 2-3 days from 24 April to 24 June 2015 and from 16 May to 08 July 2016 (67°28.766'N; 63°47.579'W; water column depth: 350 m; **Fig. 2**). Bivalves (mean wet mass \pm SE= 53.3 \pm 3.5 and 42.4 \pm 3.0 g for the truncate softshell clam (*Mya truncata*) and the Greenland cockle (*Serripes groenlandicus*) respectively; **Table S1**), were collected every 2–3 weeks from 18 January to 11 June 2015 and from 07 January to 19 June 2016, by scuba diving, at the closest coastal area from the sea ice sampling location (ca. 7.5 km west; 67°29.07'N; 63°57.92'W; **Fig. 2**).

Sea ice, sampled using a Kovacs Mark V 14 cm diameter corer focusing on the bottommost three centimeters of the core, where the bulk of ice biota occur (Smith et al., 1990), was retained for subsequent analyses of particulate organic matter (POM). To compensate for the horizontal heterogeneity of ice-algal biomass, which is typical of sea ice (Gosselin et al., 1986), sections from three or four equivalent cores were pooled in isothermal containers for each sampling. Pooled sea-ice sections were then melted with 0.2 μ m filtered seawater (FSW; 3 parts of FSW to 1 part of melted ice) to minimize osmotic stress on the microbial community during melting (Bates and Cota, 1986; Garrison and Buck, 1986) and subsequently filtered for the several analyses (i.e., lipids, Chl *a*; Sections 2.2–2.3). Sea ice core parameters (e.g., snow thickness, air temperature and photosynthetically active radiation (PAR) estimated at the bottom of sea ice) were collected during both 2015 and 2016 campaigns and have already been published elsewhere (Amiriaux et al., 2019; Massicotte et al., 2019; Oziel et al., 2019). Briefly, for each sampling date, 5–8 snow depth measurements were made with a ruler. Air temperature records were made with a meteorological station: an automated Meteo Mat equipped with temperature

sensor (HC2S3; Campbell Scientific) sensor positioned near (< 100 m) the sea ice station. Photosynthetically active radiation (PAR) below the sea ice was estimated at 1.3 m using the multispectral data collected with a Compact – Optical Profiling System (C-OPS; version Ice-PRO; Biospherical instruments Inc.; Oziel et al., 2019). To reduce the effect of sea ice surface heterogeneity on irradiance measurements (e.g., Katlein et al., 2015), the vertical attenuation coefficients of PAR were calculated by fitting a single exponential function on PAR profiles between 10 and 50 m, then used to estimate PAR at 1.3 m (more details are given by Massicotte et al., 2018). Note that 1.3 m corresponds to the highest average ice thickness measured during the two field campaigns and therefore to the first measurement under the ice (122.1 and 129.9 cm in 2015 and 2016 respectively).

After collection, bivalve samples were kept frozen (< -20°C) at the shore laboratory, before further treatment at the university laboratory. At Université Laval, bivalve individuals were freeze-dried and subsequently crushed (with exception of the shell), homogenized and kept frozen (< -20°C) prior to analysis.

2.2 Chlorophyll *a*

At the shore laboratory and within 24 h of sampling, sea ice samples originating from the pooled ice cores melted in isothermal containers were filtered in duplicates for chlorophyll *a* (Chl *a*) analyses through Whatman GF/F glass fiber filters. The Chl *a* retained on the filters was measured using a TD-700 Turner Design fluorimeter, after 18–24 h extraction in 90% acetone at 4°C in the dark (Parsons et al., 1984). The fluorimeter was calibrated with commercially available Chl *a* (*Anacystis nidulans*, Sigma).

2.3 Lipid analyses

At the shore laboratory, sea ice samples originating from pooled ice cores in isothermal containers were filtered in duplicate for lipid analyses through Whatman GF/F glass fiber filters (porosity 0.7 μm , pre-combusted 4 h at 450°C) and stored at -20°C before further treatment at the university laboratory. At Université Laval, extraction of lipids was carried out in duplicate on the algal filters (ca. 50–2500 mL filtered) and on bivalves (ca. 0.5 g dry mass). To enable HBI and fatty acid quantification, two or three internal standards were added to each sample prior to extraction. For HBI quantification, 7-hexylnonadecane (7-HND; 0.01 μg) was added to sea ice samples, while 9-octylheptadecene (9-OHD; 0.02 μg) was added to bivalve samples. For fatty acid quantification, 100 μg and 500 μg of 5 β -cholic acid were added to sea ice and bivalve samples respectively. Samples were saponified (5% KOH; 90°C, 120 min; 4 mL) in a flask, then extracted three times with hexane to recover HBI fractions and subsequently collected using open column silica chromatography (ca. 1 g silica; 6–7 mL hexane; Belt et al., 2012). The remainder of the flask was acidified with HCl to pH 1 and extracted again three times with hexane (6–7 mL hexane). The combined hexane extracts were dried over anhydrous Na_2SO_4 , filtered and concentrated to obtain the fatty acid fraction and methylated for further detection by gas chromatography-mass spectrometry (GC-MS). Analysis of lipids was carried out using GC-MS in selected ion monitoring (e.g., SIM, m/z 350 (IP_{25}), 348 (HBI IIa, b) and 346 (HBI III, IV); **Fig. 1**) mode using an Agilent 7890A series gas chromatograph ($\text{DB}_{5\text{MS}}$ fused silica column; 50 m x 0.25 mm i.d., 0.25 μm film thickness) coupled to an Agilent 5975C mass spectrometric detector (Belt et al., 2012). HBIs were identified by comparison of retention indices ($\text{RI}_{\text{DB5-MS}}$) and mass spectra to those of authentic standards (Belt, 2018; Belt et al., 2000; Tesi et al., 2020; Tesi et al., 2017). Quantification of HBIs was carried out by comparing mass spectral intensities of molecular ions to that of the internal standard and normalizing for differences in mass spectral fragmentation efficiency and volume/mass sampled. Fatty acid

quantification was made in a similar manner to that of HBIs, although using different standards (Supelco® 37 Component FAME Mix, Supelco).

2.4 Statistical analyses

2.4.1 Sea ice

Principal Component analysis (PCA) biplots of the environmental variables was used to reduce the dimensionality of the dataset using the “FactoMineR” package (Pagès, 2004). Environmental variables used into the PCA were total fatty acid (TFA), polyunsaturated fatty acid (PUFA), air temperature, PAR, snow thickness and Chl *a*, to describe the 28 and 23 sea ice sampling dates from 2015 and 2016, respectively. Wilcoxon tests were performed to test the effect of year (fixed with two levels: 2015 and 2016) on sea ice fatty acid (TFA, monounsaturated fatty acid (MUFA), PUFA, saturated fatty acid (SFA)) and HBI (IP₂₅, HBI IIa, IIb, III and IV) contents. Spearman’s rank order correlation (*r*) was used to infer the strength of associations between HBI variables and correlation significance was determined at *p-value* < 0.01.

2.4.2 Bivalves

Non-metric multidimensional scaling (nMDS), based on the Euclidean distance on normalized lipid data, was employed to graphically represent the position of the 75 bivalve specimens on the ordination diagram.

3. Results

3.1 Sea ice

On average, Chl *a* concentration in sea ice was ca. 6 times higher in 2015 than in 2016 (mean ± SE = 646.7 ± 69.4 µg L⁻¹ and 119.8 ± 17.4 µg L⁻¹, respectively; **Fig. 3**). A unique Chl *a* peak in production was observed in 2015 (May 31st; 1661.8 µg L⁻¹) while two peaks were observed in 2016 (317.3 and 306.9 µg L⁻¹ on June 1st and 13rd respectively). TFA content in sea

ice was ca. 5 times higher in 2015 than 2016 (mean \pm SE = 57.9 ± 14.0 mg L⁻¹ and 11.0 ± 2.7 mg L⁻¹, respectively; **Fig. 3, Table 1**). In 2015, the TFA maximum was observed on 15 June (332.0 mg L⁻¹; **Fig. 3, Table S2**) i.e., 15 days after the Chl *a* peak, while in 2016 it occurred on 20 June (35.2 mg L⁻¹) i.e., 7 days after the second Chl *a* peak. Fatty acid profiles of sea ice samples were dominated in both 2015 and 2016 by C_{16:1Δ7} (palmitoleic; 68.9 and 53.6% respectively) and C_{16:0} (palmitic; 26.1 and 30.8% respectively) acids; they also exhibited smaller proportions of C_{14:0} (4.7 and 4.2% respectively), C_{18:1Δ9} (oleic; 5.4 and 0.3% respectively), EPA (0.4 and 10.3% respectively) and DHA acids (0.0 and 1.2% respectively; **Table 1**). Among the TFA, the contribution of SFA (C_{14:0} and C_{16:0}) was relatively similar in 2015 and 2016 (mean \pm SE = 30.7 ± 1.9 % and 35.0 ± 2.8 %, respectively). Contributions of MUFA (palmitoleic and oleic acids) were higher in 2015 than in 2016 (mean \pm SE = 68.9 ± 2.0 % and 53.6 ± 3.2 %, respectively), while the PUFA (n-3 PUFA EPA and DHA) contribution was lower in 2015 than 2016 (mean \pm SE = 0.4 ± 0.3 % and 11.4 ± 1.9 %, respectively; **Table 1**). Absolute concentrations of the different lipid classes were significantly different between the years (Wilcoxon test; *p*-value < 10⁻⁴). Although the 2016 Spring was less productive than 2015 Spring in terms of TFA, MUFA and SFA, the PUFA content was higher (mean \pm SE = 0.9 ± 0.2 % and 0.2 ± 0.1 mg L⁻¹, respectively; **Table 1**). To unravel how sea ice sampling dates (variables) could be described by their environment (Chl *a*, snow thickness (snow), PAR, air temperature (Temperature), TFA and PUFA), a biplot PCA was performed (**Fig. 4**). The PCA accounted for 64.1% of the total variation among sea ice sampling dates (Axis 1: 44.2% and Axis 2: 19.9%). The sea ice stations (variables) are displayed according to their contribution (in %) to the dimensions of the biplot. The quality of the contribution is colored. In **Fig. 4**, contributions higher than 15 are considered as good (orange, indicator length of arrows). The analysis revealed that TFA, PAR, snow and Chl *a* are key environmental factors for describing the sea-ice sampling dates, while air temperature and PUFA are of less importance. Overall,

the 2015 sea-ice sampling stations were characterized by high snow thickness, Chl *a* and TFA concentrations associated with low PAR, air temperature and PUFA content. Conversely, the 2016 sea-ice sampling period was characterized by relatively low snow thickness and concentrations of Chl *a* and TFA associated with high PAR, air temperature and PUFA content (**Fig. 4**).

HBIs were detected during both sampling years. Because of the slightly different analytical methodology employed for the analysis of HBIs in sea-ice and bivalves, no comparison of absolute HBIs values can be made between the two types of samples. A Wilcoxon test on the different HBIs investigated showed no significant differences between 2015 and 2016 (p -value > 0.05). During both years, IP₂₅ and HBI IIa were well correlated in sea ice (Spearman's $r = 0.92$, p -value < 0.01, $n = 51$) as well as HBI IIa, III and IV (Spearman's r ranged from 0.87 to 0.94, p -value < 0.01, $n = 51$) (**Table 2**). Conversely, IP₂₅ and HBI IIa were not well correlated with HBI IIb, III or IV (**Table 2**).

3.2 Bivalves

We monitored HBIs in *M. truncata* and *S. groenlandicus* from winter to summer 2015 and 2016 (**Fig. 6**). With the exception of the four last 2015 and two last 2016 sampling dates, *M. truncata* presented higher IP₂₅ contents than *S. groenlandicus* (**Fig. 5A, B**). However, the mean IP₂₅ content of *S. groenlandicus* was higher than that of *M. truncata* in both 2015 (mean \pm SE = 127.9 \pm 63.9 and 57.0 \pm 15.9 ng g⁻¹ dry mass, respectively) and 2016 (mean \pm SE = 86.5 \pm 52.0 and 37.3 \pm 8.0 ng g⁻¹ dry mass, respectively). The IP₂₅ contents of *S. groenlandicus* collected in 2015 and 2016 presented similar seasonal trends, i.e., an exponential-like curve with low values observed from January to early May, followed by increasing values from May to late June (**Fig. 5A, B**). These increases in *S. groenlandicus* IP₂₅ content corresponded to the sea ice production period of IP₂₅. IP₂₅ content in *M. truncata* followed the same trend as *S.*

groenlandicus during both years, although the trend was not as clear (**Fig. 5A, B**). Similarly to IP₂₅, *S. groenlandicus* HBI III content was higher than in *M. truncata* in both 2015 (mean \pm SE = 19.3 \pm 4.4 and 5.3 \pm 0.8 ng g⁻¹ dry mass, respectively) and 2016 (mean \pm SD = 6.8 \pm 3.2 and 3.0 \pm 0.5 ng g⁻¹ dry mass, respectively). The HBI III contents of *S. groenlandicus* collected in 2015 and 2016 presented similar seasonal trends, i.e., low values observed from January to April/May followed by increasing values from May to late June (**Fig. 5A, B**). In both instances, the increase of *S. groenlandicus* HBI III occurred after HBI III production in sea ice and before IP₂₅ accumulation in *S. groenlandicus*. Although the general trend of low HBI III values from January to April/May followed by increasing values from May to late June was also observed for *M. truncata* (at least for 2016; **Fig. 5D**), the increase did not clearly precede that of IP₂₅; nor did it occur after sea-ice HBI production.

A strong correlation was observed between IP₂₅ and HBI IIa in *S. groenlandicus* over the two years (Spearman's $r = 0.99$, p -value < 0.01 , $n = 38$; **Table 2**). This correlation was also present, but weaker, in sea-ice POM and *M. truncata* ($r = 0.92$ and 0.44 , respectively). Correlations between HBI IIb, III and IV were strong for sea-ice POM, moderate in *S. groenlandicus* (r ranged from 0.70 to 0.87) and relatively weak in *M. truncata* (r ranged from 0.21 to 0.70).

Non-metric multidimensional scaling (nMDS) of bivalve lipid data (i.e., fatty acid and HBI contents) showed that *M. truncata* samples were well grouped, at both seasonal and interannual scales. In contrast, *S. groenlandicus* samples formed a more diffusive group at those same scales (**Fig. 6**). The fatty acid profiles of bivalves were similar to those of sea-ice POM, but occurred in different proportions (**Tables 1, 3, Table S2–S4**). For instance, *S. groenlandicus* samples during both 2015 and 2016 were dominated by EPA (mean \pm SE = 44.9 \pm 4.1 and 35.3 \pm 5.9% respectively), C_{16:0} (mean \pm SE = 20.7 \pm 1.0% and 25.6 \pm 2.7% respectively) and C_{16:1 Δ 7} acids (mean \pm SE = 15.8 \pm 1.3% and 20.0 \pm 2.9% respectively), while exhibiting lower proportions

of DHA (mean \pm SE = $8.5 \pm 0.5\%$ and $6.8 \pm 1.0\%$ respectively), C_{14:0} (mean \pm SE = 5.7 ± 0.4 and $6.9 \pm 0.6\%$ respectively) and C_{18:1 Δ 9} acid (mean \pm SE = $4.3 \pm 0.3\%$ and $5.3 \pm 0.8\%$ respectively; **Table 3**). The *M. truncata* samples during both 2015 and 2016 were dominated by EPA (mean \pm SE = $42.7 \pm 5.9\%$ and $37.4 \pm 6.0\%$ respectively), C_{16:0} (mean \pm SE = $23.8 \pm 2.5\%$ and $30.2 \pm 3.4\%$ respectively), C_{16:1 Δ 7} acids (mean \pm SE = $12.0 \pm 1.7\%$ and $16.5 \pm 3.0\%$ respectively) and DHA (mean \pm SE = $16.2 \pm 1.4\%$ and $9.3 \pm 0.8\%$ respectively). They also exhibited smaller proportions of C_{18:1 Δ 9} (mean \pm SE = 4.3 and $3.8 \pm 0.7\%$ respectively) and C_{14:0} acids (mean \pm SE = $1.9 \pm 0.3\%$ and $2.7 \pm 0.5\%$ respectively; **Table 3**). TFA contents were higher in *S. groenlandicus* than in *M. truncata* during both 2015 (mean \pm SE = 233.5 ± 19.7 and 40.1 ± 5.0 mg g⁻¹ dry mass, respectively) and 2016 (mean \pm SE = 167.6 ± 25.2 and 54.6 ± 5.0 mg g⁻¹ dry mass, respectively). Among the TFA, the contribution of SFA was relatively similar for the two species during 2015 (mean \pm SE = 25.7 ± 2.8 % and 26.4 ± 1.4 %, respectively) and 2016 (mean \pm SE = 32.9 ± 3.8 % and 32.5 ± 3.7 %, respectively), while the contribution of MUFA was slightly lower in *M. truncata* than in *S. groenlandicus* during 2015 (mean \pm SE = 15.2 ± 2.2 % and 20.1 ± 1.6 %, respectively) and 2016 (mean \pm SE = 20.3 ± 3.7 % and 25.3 ± 3.7 %, respectively; **Table 3**). Conversely, the contribution of PUFA was slightly higher in *M. truncata* than in *S. groenlandicus* during 2015 (mean \pm SE = 58.9 ± 7.2 % and 53.5 ± 4.6 %, respectively) and 2016 (mean \pm SE = 46.7 ± 6.8 % and 42.2 ± 6.9 %, respectively).

The temporal evolution of palmitoleic/palmitic acid ratios and of the TFA and PUFA contents of bivalves were monitored during both 2015 and 2016 (**Fig. 7; Table S3, S4**). Values were seasonally steady in *M. truncate*, but for TFA in *S. groenlandicus*, declined from a seasonal maximum at the beginning of sampling (**Fig. 7**). The importance of diatoms for bivalve diet was assessed here with the palmitoleic/palmitic acid ratio, which increases with the contribution of diatoms to animal biomass (Pedersen et al., 1999; Reuss and Poulsen, 2002). During both years, the ratios of *S. groenlandicus* were higher early in the sampling period (0.98

from 18 January to 21 March 2015 and 0.96 from 07 January to 10 May 2016) than afterwards (0.56 from 03 May to 26 June 2015 and 0.58 from 30 May to 19 June 2016). These low ratios corresponded to the period when bivalve consume sympagic algae (**Fig. 7A, B**). The TFA and PUFA contents of *S. groenlandicus* followed similar qualitative trends. TFA contents were highest early in the season (304.8 and 196 mg g⁻¹ dry mass in 2015 and 2016, respectively) and lowest afterwards (108.9 and 82.1 mg g⁻¹ dry mass in 2015 and 2016). For PUFA, the values declined from 180.5 and 82.7 in early 2015 and 2016, respectively, to 47.1 and 34.7 mg g⁻¹ dry subsequently (**Fig. 7C–F**).

4. Discussion

4.1 Sea ice seasonal and inter-annual lipid productivity

A Principal Component Analysis (PCA) biplot of environmental variables was used to reduce the dimensionality of the sea ice samples (**Fig. 4**). This highlighted that in 2015 the snow cover was thicker than in 2016, which resulted in reduced under-ice PAR. In terms of biomarkers, the 2015 sea ice was characterized by higher Chl *a* concentrations and TFA contents than in 2016, associated with lower PUFA (EPA and DHA) contents. The great difference in Chl *a* productivity may derive from the contrasted atmospheric forcings present during the winters preceding each sampling period. Indeed, the winter of 2014–2015 was colder and with less snowfall than the 2015–2016 winter. As a consequence, twice the amount of light was transmitted to the bottom ice prior to sampling, which could in large part explain the average six times larger sympagic production of Chl *a* in 2015 than 2016 (Oziel et al., 2019; **Fig. 3**). Since larger sympagic Chl *a* biomass was observed in 2015 than 2016, it is not surprising to also observe the largest total fatty acid production in 2015 (**Figs. 3, 4; Table 1**). Interestingly, a mismatch between TFA and Chl *a* peaks was observed over the two years (**Fig. 3**). This result has already been pointed out by Amiraux et al. (2020) during the 2016 melting

season in the same area. Those authors attributed this phenomenon to the photoacclimation of sympagic algae to higher light intensities (derived from snow melting) and the consequent reduction of their Chl *a* content per cell, resulting in a mismatch between Chl *a* and fatty acid peaks. Thus, based on the observation of Chl *a* and fatty acid peak mismatches over the two years, we suggest that this particular feature is probably common to sea ice melt.

The fatty acid profiles of the sea-ice POM obtained in southwest Baffin Bay were similar to those previously reported during spring in Svalbard and the Barents Sea (Henderson et al., 1998; Leu et al., 2011; Leu et al., 2010). However, the relative contribution of different lipid classes somewhat differed from the proportions found in the literature. PUFA contributions were notably low here (0.4 and 11.4% in 2015 and 2016 respectively) relative to those measured in Svalbard and the Barents Sea (> 17%). While the threshold percentage at which the relative contribution of a fatty acid is accounted for differ among fatty acid studies (e.g., 1 or 3%; 3% in the present study) and may have contributed to this contrast, the most likely explanation is a regional or annual difference in the relative production of fatty acids. Absolute concentrations of the different fatty acid classes greatly differed between the sampling years with higher TFA, MUFA and SFA concentration in Spring 2015 than 2016 (**Table 1**). Conversely, sympagic algae collected in Spring 2016 presented higher PUFA absolute concentrations than those of 2015 (mean \pm SE = 0.9 ± 0.2 and 0.2 ± 0.1 mg L⁻¹ in 2016 and 2015 respectively; **Table 1**; **Fig. 4**). While the total algal biomass that reaches the seafloor is important for the feeding ecology of bivalves, the nutritional value of this biomass is determined by the essential fatty acids EPA and DHA (Hendriks et al., 2003; Lane, 1987). These PUFAs are essential because most bivalve species are unable to synthesize them from shorter chain precursors (Chu and Greaves, 1991; Delaunay et al., 1993). Thus, we suggest that, although sympagic production was higher in 2015 than 2016 (as attested by e.g., Chl *a* and TFA content), the 2016 sea ice was more useful for bivalves (at least for essential fatty acids) than the 2015 production.

In a previous investigation, Amiraux et al. (2019) conducted the first analysis of the temporal evolution of IP₂₅ and other HBIs during the 2016 melting season in the same area. In the present study, sea ice HBI analysis was performed on both 2015 and 2016 samples with a different methodology and filters to those reported by Amiraux et al. (2019) in their studies. Belt et al. (2014) warned the ‘HBI scientific community’ that the absolute quantification of HBIs obtained from different laboratories and/or using different methodologies (e.g., standard: 9-OHD or 7-HND) may be relatively different. Thus, in order to prevent this bias, the present study only discusses the absolute values obtained by the same method, or else the relative values obtained from different methods (e.g., biomarker correlations).

Overall, we confirmed the general findings of Amiraux et al. (2019) for sea-ice POM; namely, the co-occurrences of: (i) IP₂₅ and HBI IIa, which is consistent with a single source (sympagic) for the two compounds (Brown et al., 2014a; Brown et al., 2014b; Limoges et al., 2018), and (ii) HBIs IIb, III and IV (**Table 2**). The latter was most likely attributed to a pelagic production at the early sea ice melts stages and within sea ice, by the tube-dwelling diatom *Berkeleya rutilens* (Amiraux et al., 2019). In recent years, numerous HBI-based proxies have been developed (Belt, 2018). Among them, the so-called PIP₂₅ index (phytoplankton marker-IP₂₅; Müller et al., 2011) has provided, in some cases, more detailed descriptions of palaeo Arctic sea-ice conditions in sediment records than using IP₂₅ alone (e.g., Belt, 2018; Berben et al., 2014; Fahl and Stein, 2012; Müller and Stein, 2014; Müller et al., 2012). On the other hand, the HBI biomarker-based ‘H-print’ has provided valuable estimates of the relative contributions of sympagic- and pelagic-derived primary production in a variety of Arctic animals (Brown, 2018; Brown et al., 2018; Brown et al., 2014d). The robustness of these proxies depends on whether the markers are unequivocally specific to sympagic and pelagic growth environments, or not. Although IP₂₅ appears to represent a suitable sympagic biomarker, due to its source specificity (Brown et al., 2014c), identification of the most suitable pelagic counterpart remains

challenging (Belt, 2018). In recent studies, the use of some other HBIs (including HBI III) has been suggested as preferable pelagic counterparts to IP₂₅, owing to their apparently greater source specificity (Belt, 2018; Belt et al., 2018; Belt et al., 2019; Köseoğlu et al., 2018; Smik, 2016). However, data from the current study confirm the findings of Amiriaux et al. (2019); namely, that HBI III can occur in sea ice and is not as specific of the pelagic environment as originally believed (**Fig. 5C, D**).

HBI production in sea-ice (including IP₂₅) did not significantly differ between years (Wilcoxon test; p -value > 0.05). Since IP₂₅-producing species are normally only present as minor components of the ice-algal assemblage (typically 1–5%; Brown et al., 2014c), the combination of a nearly stable IP₂₅-production in years with reduced ice-algal production (as indicated by the Chl *a* or TFA; **Fig. 3**) indicates a relatively high contribution of IP₂₅-producing species in 2016.

4.2. Efficiency of benthic-pelagic coupling

Pelagic–benthic coupling is known to be particularly tight on Arctic shelves (Ambrose and Renaud, 1997; Clough et al., 2005; Hobson et al., 1995; Renaud et al., 2008; Olivier et al., 2020), with a large portion (48 to 96%) of the carbon produced in the water column falling to the seafloor each year (Wassmann, 1991). Although the relative contribution of sympagic algae and phytoplankton to total marine primary production varies with ice cover and water column productivity, it has been shown that a significant fraction of the carbon reaching the seafloor derives from sympagic algal material (Belt, 2018). The joint monitoring of the sea-ice proxy IP₂₅ in both sea ice and the bivalves beneath, allowed us to determine the efficiency of the benthic-pelagic (and more precisely: benthic-sympagic) coupling for two years (**Fig. 5**). Both *M. truncata* and *S. groenlandicus* presented depleted IP₂₅ concentrations during winter months, followed by days of rapid enrichment once IP₂₅ was produced in sea ice (**Fig. 5 A, B**). This

pattern confirms that benthos rapidly responded to the influx of sympagic organic matter (days to weeks; Graf, 1989; Renaud et al., 2008). Similarly, bivalves presented depleted HBI III concentrations in winter, followed by a rapid enrichment from ca. April/May (**Fig. 5**). From its presupposed pelagic origin in the marginal ice zone (Belt et al., 2015; Collins et al., 2013; Köseoğlu et al., 2018; Smik, 2016; Smik et al., 2016b), HBI III has only been reported in phytoplankton collected during summer and autumn (Belt et al., 2017). Thus, the enrichment of HBI III in bivalves observed from ca. April/May unlikely derived from open water production. Moreover, in sea ice, the production of HBI III has been reported to occur before that of IP₂₅ (**Fig. 5**; Amiriaux et al., 2019). Thus, the earlier HBI III enrichment in bivalve flesh compared to IP₂₅ strongly supports the notion that these animals ingest sea ice-derived HBI III. Consequently, we suggest that in coastal regions at least, HBI III derived from sea ice reaches the seafloor and contributes to the diet of arctic animals, potentially lowering the robustness of the PIP₂₅ and H-print indices.

For both years, IP₂₅ and HBI III concentrations were more than twice higher in *S. groenlandicus* than in *M. truncata*. Moreover, the response of *M. truncata* to sympagic POM, as identified by their HBI enrichment (IP₂₅ and HBI III) was less evident than for *S. groenlandicus* (**Fig. 5**). An explanation may be found in the size of the organisms collected. Indeed, it has been shown that bivalve filtration rate is to some extent a function of their body size (Riisgård and Møhlenberg, 1979; Riisgård and Seerup, 2003; Sylvester et al., 2005). It follows that the consumption of large-sized sympagic algae by small bivalves should be relatively weak, resulting in a low and more variable HBI enrichment than in large bivalves. In the present study however, this argument is countered by the heavier mass of *M. truncata* samples compared to *S. groenlandicus* (**Table S1**). A more likely explanation lies in the feeding behaviors of these two bivalves. Indeed, although *S. groenlandicus* and *M. truncata* are both slow-mobile burrowing suspension feeders (Gulliksen and Svensen, 2004; Huber, 2010;

McTigue and Dunton, 2014; Shojaei, 2016), their bioturbation affinity differs. Unlike *S. groenlandicus*, *M. truncata* induces diffusive mixing bioturbation (Lacoste et al., 2018), and is expected to ingest a variable and non-negligible quantity of buried sediment. Although *M. truncata* had higher IP₂₅ content than *S. groenlandicus* during winter months (**Fig. 5A, B**), its IP₂₅ content was half that of *S. groenlandicus* over the entire season. This result supports the notion that sediment represents a non-negligible part of the diet in *M. truncata*. Indeed, the higher IP₂₅ content of *M. truncata* compared to *S. groenlandicus* in winter suggests that sediment POM represents a better source of IP₂₅ than primary production during this season. Conversely, the higher spring IP₂₅ content in *S. groenlandicus* compared to *M. truncata* suggests that primary production is the better source of IP₂₅ during this season. Moreover, since unsaturated lipids (including HBIs) are susceptible to degradative processes in the upper centimeters of the sediment (Rontani and Belt, 2019; Rontani et al., 2018), the consumption of sediment POM by *M. truncata* should provide less and more variable lipid contents (including HBI) than the supposed strict diet of sympagic and pelagic material in *S. groenlandicus*. Lipid contents (**Fig. 5, 7**) and the positive correlations between different HBIs support this interpretation (**Table 2**). Indeed, the correlations between different HBIs in *S. groenlandicus* (i.e., Spearman's $r = 0.99$ for IP₂₅ and HBI IIa; r ranged from 0.70 to 0.87 for HBI IIb, III and IV; **Table 2**) were as strong as those observed in sea ice, which attests to the almost exclusive contribution of sympagic algae to their diet during the sampling period. By contrast, the relatively weak correlations among HBIs in *M. truncata* (i.e., Spearman's $r = 0.44$ for IP₂₅ and HBI IIa; r ranged from 0.21 to 0.70 for HBI IIb, III and IV) imply a reduced sympagic contribution to their diet.

4.3. Effectiveness of essential fatty acid transfer from sea ice to bivalve

Based on lipid data, nMDS was employed to graphically represent the position of the 75 bivalves by year and species (**Fig. 6**). Unlike for *S. groenlandicus*, data for *M. truncata* samples were well clustered, suggesting low lipid variability among seasons or years. Indeed, *M. truncata* samples were distinguished from those of *S. groenlandicus* by relatively constant and lower fatty acid contents (ca. 6 and 3 times lower in 2015 and 2016 respectively; **Table 3**). This general pattern is reminiscent of that of the HBIs (as previously discussed) and reinforces the interpretation that *M. truncata* relies to a greater extent than *S. groenlandicus* on sedimentary organic matter for feeding.

Although the absolute quantities of lipid classes differed between years and bivalve species, their relative contribution was somewhat similar, with a mean PUFA (herein n-3 PUFA EPA and DHA) contribution to TFA above 40%, irrespective of species and sampling year (**Table 3**). This contribution is similar to those observed in other Arctic bivalves such as *Astarte elliptica* or *Bathyarca glacialis* (Gaillard et al., 2017; Gaillard et al., 2015) and underscores the strong accumulation of these essential plant-derived molecules in benthic filter feeders. The benthos is known to respond rapidly to the influx of sympagic organic matter (days to weeks; Graf, 1989; Renaud et al., 2008), principally due to its relatively high content in n-3 PUFAs (Arrigo and Thomas, 2004). We confirmed, through HBI analysis, that sympagic material was quickly assimilated by *M. truncata* and *S. groenlandicus* after 21 April in 2015 and after 10 May in 2016 (**Fig. 5A, B**).

Since we argued previously that sympagic/pelagic-benthic coupling is relatively weak for *M. truncate*, we will hereafter focus on *S. groenlandicus* to assess the impact of sympagic fatty acid deliveries on the quality of bivalve flesh. Diatoms represent the dominant taxon of sympagic algae (Amiriaux et al., 2019; Brown et al., 2016; Ratkova and Wassmann, 2005) and are known as good producers of EPA (Kelly and Scheibling, 2012; Viso and Marty, 1993), which was the main n-3 PUFA present in our bivalve samples (**Table 3**). It is therefore not

surprising that the palmitoleic/palmitic acid ratio, as well as the TFA and PUFA contents, were similar during both sampling years (**Fig. 7**). *S. groenlandicus* harvested before the period of peak algal production were then characterized by relatively high palmitoleic/palmitic ratios consistent with relatively strong diatom contribution to their lipid reserves. By contrast, these ratios were low in *S. groenlandicus* specimens feeding on sympagic algae (as attested by HBI measurements), at or near the apogee of the productive period in sea ice (**Table 3; Fig. 7**). While this apparent diminution of the diatom signal is unexpected at a time when ice algal deliveries to the sea floor increase, prior studies have shown that the deposition of sympagic algal biomass onto the seafloor is particularly important early in the spring when the intake of C and n-3 PUFA is required to jumpstart benthic growth and reproduction after the food limited winter (McMahon et al., 2006; North et al., 2014). Thus, these seemingly low sympagic POM intakes by bivalves result most likely from their quick utilization of this organic matter (newly delivered or previously stored), rather than from a low contribution.

The reproduction of intertidal bivalves includes gametogenesis, development and metamorphosis, all of which are energy-consuming processes (Martinez et al., 2000). The success of these processes depends on the overall physiological condition and especially the pre-spawning condition of the adults. The larger the build-up of storage material, the more weight loss the animal can incur at spawning without endangering its subsequent survival and growth (Beukema et al., 2001). In the present study, we identified the spawning period from the intake of sympagic material by the bivalves (indicated by IP₂₅ enrichment; **Fig. 5**) and the steep concurrent decrease in their fatty acid content (**Fig. 7**). Although the pre-spawning conditions were different among years and bivalve species (e.g., the initial PUFA dry mass of *S. groenlandicus* was two-fold higher from 18 January to 21 April 2015 and from 07 January to 10 May 2016 respectively), on the last sampling day of both years the two species presented similar n-3 PUFA contents, but differed in their TFA contents (**Table S3, S4**). This pattern

suggests that the n-3 PUFA content observed at the end of the sampling period represents the residual amount necessary to ensure organism survival once it has completed its spawning effort. The fact that pre-spawning n-3 PUFA and TFA contents in *M. truncata* were lower than their post-spawning values in 2015 (**Fig. 7**), suggests that the animals were then unable to acquire enough essential fatty acids for the reproductive effort, which may have been delayed or suppressed in that year.

Conclusion

We examined the contents of n-3 PUFA and HBIs of sea ice POM and two different filter-feeding bivalve species during two Arctic melting seasons that took place in southwest Baffin Bay. The results underscored a relatively strong seasonal and interannual variability in the production of organic matter (whether fatty acid or chlorophyll *a*) and biomarkers in sea ice, due to different conditions of air temperature, snow deposition and transmitted PAR. The sea ice nevertheless shared many common characteristics during the two melting seasons, including (i) a similar productivity of IP₂₅, (ii) a production of the so-called HBI pelagic biomarker HBI III that seasonally preceded that of IP₂₅, (iii) a temporal mismatch between chlorophyll *a* and fatty acid production peaks. Although Spring 2015 was the most productive for nearly all the parameters analyzed (e.g., TFA, Chl *a*), Spring 2016 was the most productive in terms of the lipids considered essential (the n-3 PUFAs EPA and DHA) for the growth and reproduction of bivalves. By tracking the different HBIs, their levels and the correlations between each of those, we (i) confirmed that sympagic-benthic coupling is tight on Arctic shelves (ii) showed that unlike *M. truncata*, *S. groenlandicus* can be used as a responsive sentinel of pelagic-benthic coupling, and (iii) confirmed that HBI III is present in sea ice, which may weaken the robustness of some HBI-based proxies. By monitoring the fatty acid content of bivalves from winter to late spring, we (i) showed that these animals greatly accumulate essential fatty acids (mean relative contributions exceeding 40%), (ii) identified their pre-spawning and post-spawning

periods, and (iii) proposed that *M. truncata* may fail to store enough essential fatty acids to support its reproductive effort in some years.

Acknowledgements

We especially thank E. Brossier for the sampling of bivalves, C. Guilmette and F. Dufour for providing preliminary lipid results. This project was made possible by the support of the hamlet of Qikiqtarjuaq and the members of the community together with the Inuksuit School and its Principal, Jacqueline Arsenault. It was conducted under the scientific coordination of the Canada Excellence Research Chair on Remote Sensing of Canada's new Arctic frontier and the CNRS & Université Laval Takuvik Joint International Laboratory (UMI3376). The field campaigns (Scientific Research License # 01 010 15N-M and # 01 001 16R-M) owed its success to the contribution of J. Ferland, G. Bécu, C. Marec, J. Lagunas, F. Bruyant, J. Larivière, E. Rehm, S. Lambert-Girard, C. Aubry, C. Lalande, A. LeBaron, C. Marty, J. Sansoulet, D. Christiansen-Stowe, A. Wells, M. Benoît-Gagné, E. Devred and M.-H. Forget from the Takuvik Laboratory, C.J. Mundy from the University of Manitoba and F. Pinczon du Sel and E. Brossier from Vagabond. We also thank the FRQNT strategic network Québec-Océan, the CCGS *Amundsen* and the Polar Continental Shelf Program for their in-kind contribution in polar logistics and scientific equipment. We especially thank C. Nozais from the Université du Québec à Rimouski for providing the sediment traps, C. Lalande (Project leader), C. Aubry, and T. Dezutter from the Université Laval Joint International Laboratory and Takuvik Laboratory for allowing the 2016 short-term sediment trap deployment. This work contributes to the scientific programs of Takuvik and Québec-Océan. We are grateful to the two anonymous reviewers, for providing helpful comments on a previous version of the manuscript.

Funding information

The first author (RA) received financial support from the Université Bretagne Loire (UBL) "post-doctoral attractiveness" program and the Sentinel North postdoctoral program of Université Laval, made possible in part by funding from the Canada First Research Excellence Fund. RA also received a postdoctoral grant from the Littoral Research Chair at Université Laval, which is mainly funded by Sentinel North and the Northern Contaminant Program of the Crown and Indigenous Relations and Northern Affairs Canada. This research was supported by the GreenEdge project, which was funded by the following French and Canadian programs and agencies: ANR (Contract #111112), CNES (project #131425), IPEV (project #1164), CSA, Foundation Total, ArcticNet, LEFE and the French Arctic Initiative (Green Edge project).

Competing interests

The authors declare that they have no competing interests.

Supplemental material

There are four pieces of supplemental material (Table S1, S2, S3, S4).

Data accessibility statement

All data are accessible at the Green Edge database (<http://www.obs-vlfr.fr/proof/php/GREENEDGE/greenedge.php>) and will be made public after publication.

Figure caption

Figure 1: Numbering system used to describe structural characteristics of highly branched isoprenoids (I) and structures of some common C₂₅ highly branched isoprenoids (IP₂₅ – IV).

Figure 2: Map of the study area with location of the station investigated in southwest Baffin Bay.

Figure 3: Time series of chlorophyll *a* and total fatty acid concentration in the bottom 0–3 cm sea ice section from (A) 25 April to 24 June 2015 and from (B) 16 May to 8 July 2016 at the sampling location in southwest Baffin Bay (Fig. 2).

Figure 4: Principal Component analysis (PCA) biplot representing the distribution of sea ice samples collected at different sampling time and year according to the environmental core variables: chlorophyll *a* (Chl *a*), snow thickness (Snow), air temperature (Temperature), photosynthetically active radiation (PAR), total fatty acid (TFA) and polyunsaturated fatty acid content (PUFA). The PCA accounts for 64.1% of the total variation among sea ice sampling dates (Axis 1: 44.2% and Axis 2: 19.9%). The environmental variables are displayed according to their contribution (%) to the dimensions of the biplot. The quality of the contribution is colored (good contribution should be higher than 15: orange, indicator length of arrow).

Figure 5: Time series of IP₂₅ (A, B) and HBI III (C, D) in sea ice (watermark) and bivalve collected from (A, C) 25 April to 24 June 2015 and from (B, D) 16 May to 8 July 2016 at the sampling location in southwest Baffin Bay (Fig. 2).

Figure 6: Non-metric multidimensional scaling (nMDS), based on the Euclidean distance on normalized lipid data (HBI and fatty acids) representing the position of the 75 bivalves collected species (*Mya truncata* or *Serripes groenlandicus*) and sampling year (2015 or 2016) on the ordination diagram. 2D stress = 0.06.

Figure 7: Time series of palmitoleic/palmitic acid ratio (A, B), total fatty acid (C, D) and polyunsaturated fatty acid content (E, F) in *Mya truncata* and *Serripes groenlandicus* collected from (A, C, E) 25 April to 24 June 2015 and from (B, D, F) 16 May to 8 July 2016 at the sampling location in southwest Baffin Bay (Fig. 2).

Table 1: Mean fatty acid composition, expressed as mass % of total fatty acids (TFA), of POM collected in the 0–3 cm of sea ice in Davis strait between 24 April to 24 June 2015 and, 16 May to 8 July 2016. Fatty acids above > 3% in at least one of the sea ice sampling investigated were included. TFA = total fatty acids expressed in mg L⁻¹; SFA = saturated fatty acid; MUFA = monounsaturated fatty acid; PUFA = polyunsaturated fatty acid. Values are means (SE).

Table 2: Correlation coefficients between chlorophyll *a* (Chl *a*) and HBI biomarkers in sea ice POM, *Serripes groenlandicus* and *Mya truncata* collected in 2015 and 2016 in southwest Baffin Bay (Fig. 2).

Table 3: Mean fatty acid composition, expressed as mass % of total fatty acids (TFA), of (A) *Serripes groenlandicus* and (B) *Mya truncata* collected in Davis strait between January and June 2015 and between January and June 2016. Fatty acids above >3% in at least one of the

bivalve sampling investigated were included. TFA = total fatty acids expressed in mg g⁻¹ dry mass; SFA = saturated fatty acid; MUFA = monounsaturated fatty acid; PUFA = polyunsaturated fatty acid. Values are mean (SE).

Table S1: Shell, wet, dry mass and dry/wet ratio of *Mya truncata* and *Serripes groenlandicus* collected in Davis strait between (A) January and June 2015 and (B) January and June 2016. Values are means (SE).

Table S2: Fatty acid composition, expressed as mass % of total fatty acids (TFA), of POM collected in the 0–3 cm of sea ice in Davis strait between 24 April to 24 June 2015 and, 16 May to 8 July 2016. Fatty acids above > 3% in at least one of the sea ice sampling investigated were included. TFA = total fatty acids expressed in mg L⁻¹; SFA = saturated fatty acid; MUFA = monounsaturated fatty acid; PUFA = polyunsaturated fatty acid. Values are means (SE).

Table S3: Fatty acid composition, expressed as mass % of total fatty acids (TFA), of (A) *Serripes groenlandicus* and (B) *Mya truncata* collected in Davis strait between January and June 2015. Fatty acids above >3% in at least one of the bivalve sampling investigated were included. TFA = total fatty acids expressed in mg g⁻¹ dry mass; SFA = saturated fatty acid; MUFA = monounsaturated fatty acid; PUFA = polyunsaturated fatty acid. Values are means (SE).

Table S4: Fatty acid composition, expressed as mass % of total fatty acids (TFA), of (A) *Serripes groenlandicus* and (B) *Mya truncata* collected in Davis strait between January and June 2016. Fatty acids above > 3% in at least one of the bivalve sampling investigated were included. TFA = total fatty acids expressed in mg g⁻¹ dry mass; SFA = saturated fatty acid; MUFA = monounsaturated fatty acid; PUFA = polyunsaturated fatty acid. Values are means (SE).

References

- Ambrose, W.G., Renaud, P.E., 1997. Does a pulsed food supply to the benthos affect polychaete recruitment patterns in the Northeast Water Polynya? *Journal of Marine Systems* 10, 483-495.
- Amiriaux, R., Belt, S.T., Vaultier, F., Galindo, V., Gosselin, M., Bonin, P., Rontani, J.-F., 2017. Monitoring photo-oxidative and salinity-induced bacterial stress in the Canadian Arctic using specific lipid tracers. *Marine Chemistry* 194, 89-99.
- Amiriaux, R., Burot, C., Bonin, P., Guasco, S., Babin, M., Rontani, J.-F., 2020. Stress factors resulting from the Arctic vernal sea ice melt: impact on the viability of the bacterial communities associated to sympagic algae. *Elementa: Science of the Anthropocene* (in press).
- Amiriaux, R., Smik, L., Köseoğlu, D., Rontani, J.-F., Galindo, V., Grondin, P.-L., Babin, M., Belt, S.T., 2019. Temporal evolution of IP₂₅ and other highly branched isoprenoid lipids in sea ice and the underlying water column during an Arctic melting season. *Elementa: Science of the Anthropocene* 7. DOI: <https://doi.org/10.1525/elementa.377>.
- Arrigo, K.R., Thomas, D.N., 2004. Large scale importance of sea ice biology in the Southern Ocean. *Antarctic Science* 16, 471-486.

- Bates, S.S., Cota, G.F., 1986. Fluorescence induction and photosynthetic responses of Arctic ice algae to sample treatment and salinity. *Journal of phycology* 22, 421-429.
- Belt, S.T., 2018. Source-specific biomarkers as proxies for Arctic and Antarctic sea ice. *Organic Geochemistry* 125, 277-298.
- Belt, S.T., Allard, W.G., Massé, G., Robert, J.-M., Rowland, S.J., 2000. Highly branched isoprenoids (HBIs): identification of the most common and abundant sedimentary isomers. *Geochimica et Cosmochimica Acta* 64, 3839-3851.
- Belt, S.T., Brown, T.A., Ampel, L., Cabedo-Sanz, P., Fahl, K., Kocis, J., Massé, G., Navarro-Rodriguez, A., Ruan, J., Xu, Y., 2014. An inter-laboratory investigation of the Arctic sea ice biomarker proxy IP₂₅ in marine sediments: key outcomes and recommendations. *Climate of the Past* 10, 155-166.
- Belt, S.T., Brown, T.A., Navarro-Rodriguez, A., Cabedo-Sanz, P., Tonkin, A., Ingle, R., 2012. A reproducible method for the extraction, identification and quantification of the Arctic sea ice proxy IP₂₅ from marine sediments. *Analytical Methods* 4, 705-713.
- Belt, S.T., Brown, T.A., Smik, L., Assmy, P., Mundy, C., 2018. Sterol identification in floating Arctic sea ice algal aggregates and the Antarctic sea ice diatom *Berkeleya adeliensis*. *Organic geochemistry* 118, 1-3.
- Belt, S.T., Brown, T.A., Smik, L., Tatarek, A., Wiktor, J., Stowasser, G., Assmy, P., Allen, C.S., Husum, K., 2017. Identification of C₂₅ highly branched isoprenoid (HBI) alkenes in diatoms of the genus *Rhizosolenia* in polar and sub-polar marine phytoplankton. *Organic Geochemistry* 110, 65-72.
- Belt, S.T., Cabedo-Sanz, P., Smik, L., Navarro-Rodriguez, A., Berben, S.M.P., Knies, J., Husum, K., 2015. Identification of paleo Arctic winter sea ice limits and the marginal ice zone: Optimised biomarker-based reconstructions of late Quaternary Arctic sea ice. *Earth and Planetary Science Letters* 431, 127-139.
- Belt, S.T., Massé, G., Rowland, S.J., Poulin, M., Michel, C., LeBlanc, B., 2007. A novel chemical fossil of palaeo sea ice: IP₂₅. *Organic Geochemistry* 38, 16-27.
- Belt, S.T., Smik, L., Brown, T.A., Kim, J.H., Rowland, S.J., Allen, C.S., Gal, J.K., Shin, K.H., Lee, J.I., Taylor, K.W.R., 2016. Source identification and distribution reveals the potential of the geochemical Antarctic sea ice proxy IPSO₂₅. *Nature Communications* 7. DOI: <https://doi.org/10.1038/ncomms12655>.
- Belt, S.T., Smik, L., Köseoğlu, D., Knies, J., Husum, K., 2019. A novel biomarker-based proxy for the spring phytoplankton bloom in Arctic and sub-arctic settings—HBI T₂₅. *Earth and Planetary Science Letters* 523, 115703.
- Berben, S., Husum, K., Cabedo-Sanz, P., Belt, S., 2014. Holocene sub-centennial evolution of Atlantic water inflow and sea ice distribution in the western Barents Sea. *Climate of the Past* 10, 181-198.
- Beukema, J., Drent, J., Honkoop, P., 2001. Maximizing lifetime egg production in a Wadden Sea population of the tellinid bivalve *Macoma balthica*: a trade-off between immediate and future reproductive outputs. *Marine Ecology Progress Series* 209, 119-129.

- Boetius, A., Albrecht, S., Bakker, K., Bienhold, C., Felden, J., Fernández-Méndez, M., Hendricks, S., Katlein, C., Lalande, C., Krumpfen, T., Nicolaus, M., Peeken, I., Rabe, B., Rogacheva, A., Rybakova, E., Somavilla, R., Wenzhöfer, F., Party, R.P.A.-S.S., 2013. Export of Algal Biomass from the Melting Arctic Sea Ice. *Science* 339, 1430-1432.
- Brown, T., Alexander, C., Yurkowski, D., Ferguson, S., Belt, S., 2014a. Identifying variable sea ice carbon contributions to the Arctic ecosystem: A case study using highly branched isoprenoid lipid biomarkers in Cumberland Sound ringed seals. *Limnology and oceanography* 59, 1581-1589.
- Brown, T.A., 2018. Stability of the lipid biomarker H-Print within preserved animals. *Polar Biology* 41, 1901-1905.
- Brown, T.A., Assmy, P., Hop, H., Wold, A., Belt, S.T., 2017. Transfer of ice algae carbon to ice-associated amphipods in the high-Arctic pack ice environment. *Journal of Plankton Research* 39, 664-674.
- Brown, T.A., Belt, S.T., 2012. Identification of the sea ice diatom biomarker IP₂₅ in Arctic benthic macrofauna: direct evidence for a sea ice diatom diet in Arctic heterotrophs. *Polar Biology* 35, 131-137.
- Brown, T.A., Belt, S.T., Cabedo-Sanz, P., 2014b. Identification of a novel di-unsaturated C₂₅ highly branched isoprenoid in the marine tube-dwelling diatom *Berkeleya rutilans*. *Environmental Chemistry Letters* 12, 455-460.
- Brown, T.A., Belt, S.T., Gosselin, M., Levasseur, M., Poulin, M., Mundy, C.J., 2016. Quantitative estimates of sinking sea ice particulate organic carbon based on the biomarker IP₂₅. *Marine Ecology Progress Series* 546, 17-29.
- Brown, T.A., Belt, S.T., Tatarek, A., Mundy, C.J., 2014c. Source identification of the Arctic sea ice proxy IP₂₅. *Nature Communications* 5. DOI: <https://doi.org/10.1038/ncomms5197>.
- Brown, T.A., Galicia, M.P., Thiemann, G.W., Belt, S.T., Yurkowski, D.J., Dyck, M.G., 2018. High contributions of sea ice derived carbon in polar bear (*Ursus maritimus*) tissue. *PloS one* 13, e0191631.
- Brown, T.A., Yurkowski, D.J., Ferguson, S.H., Alexander, C., Belt, S.T., 2014d. H-Print: a new chemical fingerprinting approach for distinguishing primary production sources in Arctic ecosystems. *Environmental Chemistry Letters* 12, 387-392.
- Chu, F.-L., Greaves, J., 1991. Metabolism of palmitic, linoleic, and linolenic acids in adult oysters, *Crassostrea virginica*. *Marine Biology* 110, 229-236.
- Clough, L.M., Renaud, P.E., Ambrose Jr, W.G., 2005. Impacts of water depth, sediment pigment concentration, and benthic macrofaunal biomass on sediment oxygen demand in the western Arctic Ocean. *Canadian Journal of Fisheries and Aquatic Sciences* 62, 1756-1765.
- Collins, L.G., Allen, C.S., Pike, J., Hodgson, D.A., Weckström, K., Massé, G., 2013. Evaluating highly branched isoprenoid (HBI) biomarkers as a novel Antarctic sea-ice proxy in deep ocean glacial age sediments. *Quaternary Science Reviews* 79, 87-98.

- Delaunay, F., Marty, Y., Moal, J., Samain, J.-F., 1993. The effect of monospecific algal diets on growth and fatty acid composition of *Pecten maximus* (L.) larvae. *Journal of Experimental Marine Biology and Ecology* 173, 163-179.
- Dupont, F., 2012. Impact of sea-ice biology on overall primary production in a biophysical model of the pan-Arctic Ocean. *Journal of Geophysical Research: Oceans* 117. DOI: <https://doi.org/10.1029/2011JC006983>.
- Fahl, K., Stein, R., 2012. Modern seasonal variability and deglacial/Holocene change of central Arctic Ocean sea-ice cover: New insights from biomarker proxy records. *Earth and Planetary Science Letters* 351-352, 123-133.
- Falk-Petersen, S., Sargent, J.R., Henderson, J., Hegseth, E.N., Hop, H., Okolodkov, Y.B., 1998. Lipids and fatty acids in ice algae and phytoplankton from the Marginal Ice Zone in the Barents Sea. *Polar Biology* 20, 41-47.
- Fernández-Méndez, M., Katlein, C., Rabe, B., Nicolaus, M., Peeken, I., Bakker, K., Flores, H., Boetius, A., 2015. Photosynthetic production in the central Arctic Ocean during the record sea-ice minimum in 2012. *Biogeosciences* 12, 3525-3549.
- Gaillard, B., Meziane, T., Tremblay, R., Archambault, P., Blicher, M.E., Chauvaud, L., Rysgaard, S., Olivier, F., 2017. Food resources of the bivalve *Astarte elliptica* in a sub-Arctic fjord: a multi-biomarker approach. *Marine Ecology Progress Series* 567, 139-156.
- Gaillard, B., Meziane, T., Tremblay, R., Archambault, P., Layton, K.K., Martel, A.L., Olivier, F., 2015. Dietary tracers in *Batharca glacialis* from contrasting trophic regions in the Canadian Arctic. *Marine Ecology Progress Series* 536, 175-186.
- Garrison, D.L., Buck, K.R., 1986. Organism losses during ice melting: A serious bias in sea ice community studies. *Polar Biology* 6, 237-239.
- Gosselin, M., Legendre, L., Therriault, J.C., Demers, S., Rochet, M., 1986. Physical control of the horizontal patchiness of sea ice microalgae. *Marine Ecology Progress Series* 29, 289-298.
- Gosselin, M., Levasseur, M., Wheeler, P.A., Horner, R.A., Booth, B.C., 1997. New measurements of phytoplankton and ice algal production in the Arctic Ocean. *Deep Sea Research Part II* 44, 1623-1644.
- Graf, G., 1989. Benthic-pelagic coupling in a deep-sea benthic community. *Nature* 341, 437.
- Gulliksen, B., Svensen, E., 2004. Svalbard and life in polar oceans. Kom forlag, Kristiansund, Norway. ISBN: 8292496033.
- Harning, D.J., Jennings, A.E., Köseoğlu, D., Belt, S.T., Geirsdóttir, Á., Sepúlveda, J., 2020. Response of biological productivity to North Atlantic marine front migration during the Holocene. *Climate of the Past Discussions*, 1-26.
- Henderson, R., Hegseth, E., Park, M., 1998. Seasonal variation in lipid and fatty acid composition of ice algae from the Barents Sea. *Polar Biology* 20, 48-55.

- Hendriks, I.E., van Duren, L.A., Herman, P.M., 2003. Effect of dietary polyunsaturated fatty acids on reproductive output and larval growth of bivalves. *Journal of Experimental Marine Biology and Ecology* 296, 199-213.
- Hobson, K.A., Ambrose Jr, W.G., Renaud, P.E., 1995. Sources of primary production, benthic-pelagic coupling, and trophic relationships within the Northeast Water Polynya: insights from $d^{13}C$ and $d^{15}N$ analysis. *Marine Ecology Progress Series* 128, 1-10.
- Horner, R., Schrader, G., 1982. Relative contributions of ice algae, phytoplankton, and benthic microalgae to primary production in nearshore regions of the Beaufort Sea. *Arctic*, 485-503.
- Huber, M., 2010. *Compendium of Bivalves*. ConchBooks, Hackenheim.
- Katlein, C., Arndt, S., Nicolaus, M., Perovich, D.K., Jakuba, M.V., Suman, S., Elliott, S., Whitcomb, L.L., McFarland, C.J., Gerdes, R., 2015. Influence of ice thickness and surface properties on light transmission through Arctic sea ice. *Journal of Geophysical Research: Oceans* 120, 5932-5944.
- Kelly, J.R., Scheibling, R.E., 2012. Fatty acids as dietary tracers in benthic food webs. *Marine Ecology Progress Series*, 446, 1-22.
- Köseoğlu, D., Belt, S.T., Smik, L., Yao, H., Panieri, G., Knies, J., 2018. Complementary biomarker-based methods for characterising Arctic sea ice conditions: A case study comparison between multivariate analysis and the PIP_{25} index. *Geochimica et Cosmochimica Acta* 222, 406-420.
- Lacoste, É., Piot, A., Archambault, P., McKindsey, C.W., Nozais, C., 2018. Bioturbation activity of three macrofaunal species and the presence of meiofauna affect the abundance and composition of benthic bacterial communities. *Marine Environmental Research* 136, 62-70.
- Lane, A.J., 1987. The effect of a microencapsulated fatty acid diet on larval production in the European flat oyster *Ostrea edulis* L. University of Wales (UCNW, Bangor: Ocean Sciences).
- Leonardos, N., Lucas, I.A., 2000. The nutritional value of algae grown under different culture conditions for *Mytilus edulis* L. larvae. *Aquaculture* 182, 301-315.
- Leu, E., Søreide, J.E., Hessen, D.O., Falk-Petersen, S., Berge, J., 2011. Consequences of changing sea-ice cover for primary and secondary producers in the European Arctic shelf seas: Timing, quantity, and quality. *Progress in Oceanography* 90, 18-32.
- Leu, E., Wiktor, J., Søreide, J.E., Berge, J., Falk-Petersen, S., 2010. Increased irradiance reduces food quality of sea ice algae. *Marine Ecology Progress Series* 411, 49-60.
- Limoges, A., Massé, G., Weckström, K., Poulin, M., Ellegaard, M., Heikkilä, M., Geilfus, N.-X., Sejr, M.K., Rysgaard, S., Ribeiro, S., 2018. Spring Succession and Vertical Export of Diatoms and IP_{25} in a Seasonally Ice-Covered High Arctic Fjord. *Frontiers in Earth Science* 6, 226.
- Lovvorn, J.R., Cooper, L.W., Brooks, M.L., De Ruyck, C.C., Bump, J.K., Grebmeier, J.M., 2005. Organic matter pathways to zooplankton and benthos under pack ice in late winter and

open water in late summer in the north-central Bering Sea. *Marine Ecology Progress Series* 291, 135-150.

Martinez, G., Brokordt, K., Aguilera, C., Soto, V., Guderley, H., 2000. Effect of diet and temperature upon muscle metabolic capacities and biochemical composition of gonad and muscle in *Argopecten purpuratus* Lamarck 1819. *Journal of Experimental Marine Biology and Ecology* 247, 29-49.

Massé, G., Belt, S.T., Crosta, X., Schmidt, S., Snape, I., Thomas, D.N., Rowland, S.J., 2011. Highly branched isoprenoids as proxies for variable sea ice conditions in the Southern Ocean. *Antarctic Science* 23, 487-498.

Massicotte, P., Amiraux, R., Amyot, M.-P., Archambault, P., Ardyna, M., Arnaud, L., Artigue, L., Aubry, C., Ayotte, P., Bécu, G., 2019. Green Edge ice camp campaigns: understanding the processes controlling the under-ice Arctic phytoplankton spring bloom. *Earth System Science Data* 12, 151–176.

Massicotte, P., Bécu, G., Lambert-Girard, S., Leymarie, E., Babin, M., 2018. Estimating underwater light regime under spatially heterogeneous sea ice in the Arctic. *Applied Sciences* 8, 2693.

McMahon, K.W., Ambrose Jr, W.G., Johnson, B.J., Yi Sun, M., Lopez, G.R., Clough, L.M., Carroll, M.L., 2006. Benthic community response to ice algae and phytoplankton in Ny Ålesund, Svalbard. *Marine Ecology Progress Series* 310, 1-14.

McTigue, N.D., Dunton, K.H., 2014. Trophodynamics and organic matter assimilation pathways in the northeast Chukchi Sea, Alaska. *Deep Sea Research Part II: Topical Studies in Oceanography* 102, 84-96.

Morata, N., Renaud, P.E., 2008. Sedimentary pigments in the western Barents Sea: A reflection of pelagic-benthic coupling? *Deep Sea Research Part II: Topical Studies in Oceanography* 55, 2381-2389.

Müller, J., Stein, R., 2014. High-resolution record of late glacial and deglacial sea ice changes in Fram Strait corroborates ice–ocean interactions during abrupt climate shifts. *Earth and Planetary Science Letters* 403, 446-455.

Müller, J., Wagner, A., Fahl, K., Stein, R., Prange, M., Lohmann, G., 2011. Towards quantitative sea ice reconstructions in the northern North Atlantic: A combined biomarker and numerical modelling approach. *Earth and Planetary Science Letters* 306, 137-148.

Müller, J., Werner, K., Stein, R., Fahl, K., Moros, M., Jansen, E., 2012. Holocene cooling culminates in sea ice oscillations in Fram Strait. *Quaternary Science Reviews* 47, 1-14.

Napolitano, G.E., Ackman, R.G., Ratnayake, W.M., 1990. Fatty acid composition of three cultured algal species (*isochrysis galbana*, *chaetoceros gracilis* and *chaetoceros calcitrans*) used as food for bivalve larvae. *Journal of the World Aquaculture Society* 21, 122-130.

North, C.A., Lovvorn, J.R., Kolts, J.M., Brooks, M.L., Cooper, L.W., Grebmeier, J.M., 2014. Deposit-feeder diets in the Bering Sea: potential effects of climatic loss of sea ice-related microalgal blooms. *Ecological applications* 24, 1525-1542.

Olivier, F., Gaillard, B., Thébault, J., Meziane, T., Tremblay, R., Dumont, D., S, B., Gosselin, M., Jolivet, A., Chauvaud, L., Martel, A.L., Rysgaard, S., Olivier, A.-H., Pettré, J., Mars, J., Gerber, S., Archambault, P., 2020. Shells of the bivalve *Astarte moerchi* give new evidence of a strong pelagic-benthic coupling's shift occurring since the late 70s in the NOW Polynya. *Philosophical Transactions of the Royal Society A*, 378 (2181), 20190353.

Oziel, L., Massicotte, P., Randelhoff, A., Ferland, J., Vladioiu, A., Lacour, L., Lambert-Girard, S., Dumont, D., Cuypers, Y., Bouruet-Aubertot, P., Galindo, V., Marec, C., Forget, M.-H., Garcia, N., Raimbault, P., Houssais, M.-N., Babin, M., 2019. Environmental factors influencing the seasonal dynamics of under-ice spring blooms in Baffin Bay. *Elementa: Science of the Anthropocene*, 7(1), 34.

Pabi, S., van Dijken, G.L., Arrigo, K.R., 2008. Primary production in the Arctic Ocean, 1998–2006. *Journal of Geophysical Research: Oceans* 113. DOI: <https://doi.org/10.1029/2007JC004578>.

Pagès, J., 2004. Analyse factorielle de données mixtes: principe et exemple d'application. *Revue de Statistique Appliquée* LII, 93–111.

Parsons, T., Maita, Y., Lalli, C., 1984. A manual of chemical and biological methods for seawater analysis. Pergamon Press, Totronto. ISBN: 0080302874.

Pedersen, L., Jensen, H.M., Burmeister, A., Hansen, B.W., 1999. The significance of food web structure for the condition and tracer lipid content of juvenile snail fish (Pisces: *Liparis spp.*) along 65–72°N off West Greenland. *Journal of Plankton Research* 21, 1593–1611.

Poulin, M., Daugbjerg, N., Gradinger, R., Ilyash, L., Ratkova, T., von Quillfeldt, C., 2011. The pan-Arctic biodiversity of marine pelagic and sea-ice unicellular eukaryotes: a first-attempt assessment. *Marine Biodiversity* 41, 13–28.

Ratkova, T.N., Wassmann, P., 2005. Sea ice algae in the White and Barents seas: composition and origin. *Polar Research* 24, 95–110.

Renaud, P.E., Morata, N., Carroll, M.L., Denisenko, S.G., Reigstad, M., 2008. Pelagic-benthic coupling in the western Barents Sea: Processes and time scales. *Deep Sea Research Part II: Topical Studies in Oceanography* 55, 2372–2380.

Reuss, N., Poulsen, L., 2002. Evaluation of fatty acids as biomarkers for a natural plankton community. A field study of a spring bloom and a post-bloom period off West Greenland. *Marine Biology* 141, 423–434.

Riebesell, U., Schloss, I., Smetacek, V., 1991. Aggregation of algae released from melting sea ice - Implications for seeding and sedimentation. *Polar Biology* 11, 239–248.

Riisgård, H.U., Møhlenberg, F., 1979. An improved automatic recording apparatus for determining the filtration rate of *Mytilus edulis* as a function of size and algal concentration. *Marine Biology* 52, 61–67.

Riisgård, H.U., Seerup, D.F., 2003. Filtration rates in the soft clam *Mya arenaria*: effects of temperature and body size. *Sarsia* 88, 416–428.

- Rontani, J.-F., Belt, S.T., 2019. Photo-and autoxidation of unsaturated algal lipids in the marine environment: an overview of processes, their potential tracers, and limitations. *Organic Geochemistry* 139, 103941.
- Rontani, J.-F., Belt, S.T., Amiriaux, R., 2018. Biotic and abiotic degradation of the sea ice diatom biomarker IP₂₅ and selected algal sterols in near-surface Arctic sediments. *Organic Geochemistry* 118, 73-88.
- Roy, V., Iken, K., Gosselin, M., Tremblay, J.-É., Bélanger, S., Archambault, P., 2015. Benthic faunal assimilation pathways and depth-related changes in food-web structure across the Canadian Arctic. *Deep Sea Research Part I: Oceanographic Research Papers* 102, 55-71.
- Shojaei, M., 2016. Developments in German Bight benthic ecology driven by climate change and anthropogenic utilisation. Doctoral dissertation, University Bremen, Germany.
- Smik, L., 2016. Development of biomarker-based proxies for paleo sea-ice reconstructions. Doctoral dissertation, University of Plymouth, United Kingdom.
- Smik, L., Belt, S.T., Lieser, J.L., Armand, L.K., Leventer, A., 2016a. Distributions of highly branched isoprenoid alkenes and other algal lipids in surface waters from East Antarctica: Further insights for biomarker-based paleo sea-ice reconstruction. *Organic Geochemistry* 95, 71-80.
- Smik, L., Cabedo-Sanz, P., Belt, S.T., 2016b. Semi-quantitative estimates of paleo Arctic sea ice concentration based on source-specific highly branched isoprenoid alkenes: A further development of the PIP₂₅ index. *Organic Geochemistry* 92, 63-69.
- Smith, S.D., Muench, R.D., Pease, C.H., 1990. Polynyas and leads: An overview of physical processes and environment. *Journal of Geophysical Research: Oceans* 95, 9461-9479.
- Søreide, J.E., Falk-Petersen, S., Hegseth, E.N., Hop, H., Carroll, M.L., Hobson, K.A., Blachowiak-Samolyk, K., 2008. Seasonal feeding strategies of *Calanus* in the high-Arctic Svalbard region. *Deep Sea Research Part II: Topical Studies in Oceanography* 55, 2225-2244.
- Sun, M.-Y., Clough, L.M., Carroll, M.L., Dai, J., Ambrose Jr, W.G., Lopez, G.R., 2009. Different responses of two common Arctic macrobenthic species (*Macoma balthica* and *Monoporeia affinis*) to phytoplankton and ice algae: Will climate change impacts be species specific? *Journal of Experimental Marine Biology and Ecology* 376, 110-121.
- Sylvester, F., Dorado, J., Boltovskoy, D., Juárez, Á., Cataldo, D., 2005. Filtration rates of the invasive pest bivalve *Limnoperna fortunei* as a function of size and temperature. *Hydrobiologia* 534, 71-80.
- Tesi, T., Belt, S., Gariboldi, K., Muschitiello, F., Smik, L., Finocchiaro, F., Giglio, F., Colizza, E., Gazzurra, G., Giordano, P., 2020. Resolving sea ice dynamics in the north-western Ross Sea during the last 2.6 ka: From seasonal to millennial timescales. *Quaternary Science Reviews* 237, 106299.
- Tesi, T., Geibel, M.C., Pearce, C., Panova, E., Vonk, J.E., Karlsson, E., Salvado, J.A., Kruså, M., Bröder, L., Humborg, C., Semiletov, I., Gustafsson, Ö., 2017. Carbon geochemistry of plankton-dominated samples in the Laptev and East Siberian shelves: contrasts in suspended particle composition. *Ocean Science* 13, 735-748.

- van der Loeff, M.R., Meyer, R., Rudels, B., Rachor, E., 2002. Resuspension and particle transport in the benthic nepheloid layer in and near Fram Strait in relation to faunal abundances and ^{234}Th depletion. *Deep Sea Research Part I: Oceanographic Research Papers* 49, 1941-1958.
- Viso, A.-C., Marty, J.-C., 1993. Fatty acids from 28 marine microalgae. *Phytochemistry* 34, 1521-1533.
- Volkman, J.K., Jeffrey, S.W., Nichols, P.D., Rogers, G.I., Garland, C.D., 1989. Fatty acid and lipid composition of 10 species of microalgae used in mariculture. *Journal of Experimental Marine Biology and Ecology* 128, 219-240.
- Wang, S.W., Budge, S.M., Gradinger, R.R., Iken, K., Wooller, M.J., 2014. Fatty acid and stable isotope characteristics of sea ice and pelagic particulate organic matter in the Bering Sea: tools for estimating sea ice algal contribution to Arctic food web production. *Oecologia* 174, 699-712.
- Wassmann, P., 1991. Dynamics of primary production and sedimentation in shallow fjords and pols of western Norway. *Oceanography and Marine Biology Annual Review* 29, 87-154.
- Wassmann, P., Duarte, C.M., Agustí, S., Sejr, M.K., 2011. Footprints of climate change in the Arctic marine ecosystem. *Global Change Biology* 17, 1235-1249.

Table 1: Mean fatty acid composition, expressed as mass % of total fatty acids (TFA), of POM collected in the 0–3 cm of sea ice in Davis strait between 24 April to 24 June 2015 and, 16 May to 8 July 2016. Fatty acids above > 3% in at least one of the sea ice sampling investigated were included. TFA = total fatty acids expressed in mg L⁻¹; SFA = saturated fatty acid; MUFA = monounsaturated fatty acid; PUFA = polyunsaturated fatty acid. Values are mean (SE).

Fatty acid	Sea ice sampling year	
	2015	2016
14:00	4.7 (0.4)	4.2 (0.3)
16:00	26.1 (1.9)	30.8 (2.8)
∑SFA	30.7 (1.9)	35.0 (2.8)
16:1 ω 7	68.9 (2.0)	53.6 (3.2)
18:1 ω 9	5.4 (0.1)	0.3 (0.1)
∑MUFA	68.9 (2.0)	53.6 (3.2)
EPA	0.5 (0.3)	10.3 (1.7)
DHA	0.0 (0.0)	1.2 (0.3)
∑PUFA	0.4 (0.3)	11.4 (1.9)
TFA ^a	57.9 (14.0)	11.0 (2.7)

^a Expressed in mg L⁻¹

Table 2: Correlation coefficients between chlorophyll *a* (Chl *a*) and HBI biomarkers in sea ice POM, *Serripes groenlandicus* and *Mya truncata* collected in 2015 and 2016 in Davis Strait (Figure 2).

Sample type	Factor	Chl <i>a</i>	IP ₂₅	HBI IIa	HBI IIb	HBI III
Sea ice POM (n = 51)	Chl <i>a</i>	1	– ^b	–	–	–
	IP ₂₅	0.58* ^a	1	–	–	–
	HBI IIa	0.61*	0.92*	1	–	–
	HBI IIb	n/a ^c	0.27	0.34	1	–
	HBI III	0.39*	0.32	0.39*	0.88*	1
	HBI IV	0.45*	0.41*	0.47*	0.87*	0.94*
<i>Serripes groenlandicus</i> (n = 38)	IP ₂₅	n/a	1	–	–	–
	HBI IIa	n/a	0.99*	1	–	–
	HBI IIb	n/a	0.74*	0.79*	1	–
	HBI III	n/a	0.62*	0.64*	0.72*	1
	HBI IV	n/a	0.69*	0.72*	0.70*	0.87*
<i>Mya truncata</i> (n = 38)	IP ₂₅	n/a	1	–	–	–
	HBI IIa	n/a	0.44*	1	–	–
	HBI IIb	n/a	0.60*	0.39*	1	–
	HBI III	n/a	0.71*	0.15	0.60*	1
	HBI IV	n/a	0.37*	0.71*	0.70*	0.21*

^aAsterisk indicates significant correlation: $p < 0.01$.

^bRepetition of value.

^cNot applicable.

Table 3: Mean fatty acid composition, expressed as mass % of total fatty acids (TFA), of (A) *Serripes groenlandicus* and (B) *Mya truncata* collected in Davis strait between January and June 2015 and between January and June 2016. Fatty acids above >3% in at least one of the bivalve sampling investigated were included. TFA = total fatty acids expressed in mg g⁻¹ dry mass; SFA = saturated fatty acid; MUFA = monounsaturated fatty acid; PUFA = polyunsaturated fatty acid. Values are mean (SE).

Fatty acid	<i>Mya truncata</i> sampling year		<i>Serripes groenlandicus</i> sampling year	
	2015	2016	2015	2016
14:00	1.9 (0.3)	2.7 (0.5)	5.7 (0.4)	6.9 (0.6)
16:00	23.8 (2.5)	30.2 (3.4)	20.7 (1.0)	25.6 (2.7)
∑SFA	25.7 (2.8)	32.9 (3.8)	26.4 (1.4)	32.5 (3.3)
16:1ω7	12.0 (1.7)	16.5 (3.0)	15.8 (1.3)	20.0 (2.9)
18:1ω9	3.3 (0.5)	3.8 (0.7)	4.3 (0.3)	5.3 (0.8)
∑MUFA	15.3 (2.2)	20.3 (3.7)	20.1 (1.6)	25.3 (3.7)
EPA	42.7 (5.9)	37.4 (6.0)	44.9(4.1)	35.3 (5.9)
DHA	16.2 (1.4)	9.3 (0.8)	8.5 (0.5)	6.8 (1.0)
∑PUFA	58.9 (7.2)	46.7 (6.8)	53.5 (4.6)	42.2 (6.9)
TFA ^a	40.1 (5.0)	54.6 (11.0)	233.5 (19.7)	167.6 (25.2)

^a Expressed in mg L⁻¹

Declaration of interests

The authors declare that they have no known competing financial interests or personal relationships that could have appeared to influence the work reported in this paper.

The authors declare the following financial interests/personal relationships which may be considered as potential competing interests:

Journal Pre-proofs

Highlights

- Spring sea ice has strong interannual IP₂₅, TFA and PUFA production variability
- Production of the 'pelagic' biomarker HBI III observed in sea ice
- Incorporation of sea ice-derived HBI III observed in bivalves
- *S. groenlandicus* is a responsive sentinel of Arctic sympagic-benthic coupling
- *M. truncata* did not store enough essential fatty acids to support reproduction

Journal Pre-proofs